Ly6C^{Hi} Blood Monocyte/Macrophage Drive Chronic Inflammation and Impair Wound Healing in Diabetes Mellitus

Andrew Kimball, Matthew Schaller, Amrita Joshi, Frank M. Davis, Aaron denDekker, Anna Boniakowski, Jennifer Bermick, Andrea Obi, Bethany Moore, Peter K. Henke, Steve L. Kunkel, Katherine A. Gallagher

Objective—Wound monocyte-derived macrophage plasticity controls the initiation and resolution of inflammation that is critical for proper healing, however, in diabetes mellitus, the resolution of inflammation fails to occur. In diabetic wounds, the kinetics of blood monocyte recruitment and the mechanisms that control in vivo monocyte/macrophage differentiation remain unknown.

Approach and Results—Here, we characterized the kinetics and function of Ly6C^{Hi} [Lin$^-$ (CD3$^-$CD19$^-$NK1.1$^-$Ter-119$^-$) Ly6G$^-$CD11b$^+$] and Ly6C^{Lo} [Lin$^-$ (CD3$^-$CD19$^-$NK1.1$^-$Ter-119$^-$) Ly6G$^-$CD11b$^+$] monocyte/macrophage subsets in normal and diabetic wounds. Using flow-sorted *tdTomato*-labeled Ly6C^{Hi} monocyte/macrophages, we show Ly6C^{Hi} cells transition to a Ly6C^{Lo} phenotype in normal wounds, whereas in diabetic wounds, there is a late, second influx of Ly6C^{Hi} cells that fail transition to Ly6C^{Lo}. The second wave of Ly6C^{Hi} cells in diabetic wounds corresponded to a spike in MCP-1 (monocyte chemoattractant protein-1) and selective administration of anti-MCP-1 reversed the second Ly6C^{Hi} influx and improved wound healing. To examine the in vivo phenotype of wound monocyte/macrophages, RNA-seq–based transcriptome profiling was performed on flow-sorted Ly6C^{Hi} [Lin$^-$Ly6G$^-$CD11b$^+$] and Ly6C^{Lo} [Lin$^-$Ly6G$^-$CD11b$^+$] cells from normal and diabetic wounds. Gene transcriptome profiling of diabetic wound Ly6C^{Hi} cells demonstrated differences in proinflammatory and profibrotic genes compared with controls.

Conclusions—Collectively, these data identify kinetic and functional differences in diabetic wound monocyte/macrophages and demonstrate that selective targeting of CD11b$^+$Ly6C^{Hi} monocyte/macrophages is a viable therapeutic strategy for inflammation in diabetic wounds.

Visual Overview—An online visual overview is available for this article. **(*Arterioscler Thromb Vasc Biol*. 2018;38: 1102-1114. DOI: 10.1161/ATVBAHA.118.310703.)**

Key Words: diabetes mellitus ■ inflammation ■ macrophages ■ monocytes ■ wound healing

Impaired wound healing in diabetes mellitus is presently the leading cause of lower extremity amputation in the United States and costs the healthcare system >$19 billion dollars annually. Importantly, amputation is associated with a 50% mortality rate at 5 years, a survival rate worse than most cancers.[1,2] Impaired wound healing in diabetes mellitus is multifactorial because of a combination of peripheral artery disease, peripheral neuropathy, inflammation, and altered immune cell function.[3] Peripheral artery disease is present in over half of patients with diabetic wounds and contributes significantly to impaired healing.[4] Persistent, uncoordinated inflammation is a hallmark of chronic nonhealing wounds in diabetes mellitus.[5] Our laboratory and others have found increased inflammatory macrophages in diabetic wounds when anti-inflammatory macrophages should predominate to help drive tissue repair, however, the mechanisms that sustain the inflammatory macrophage phenotype in diabetic wounds has not been identified.[5–12]

The recruitment of circulating blood monocytes to the site of tissue injury plays a critical role in tissue repair through the coordination of inflammation. The precise timing of both the initiation and resolution of inflammation is essential for restoring tissue integrity. The first phase of the inflammatory response is destructive to the tissue and promotes clearance of invading pathogens, whereas the second phase is a resolution phase where tissue repair ensues.[13,14] For this reason, inflammation is an adaptive process that is necessary to maintain tissue homeostasis.[15–17] In the absence of precise programmed inflammation, pathological nonhealing ensues.[6,10,18–20]

Infiltrating blood monocyte-derived macrophages (monocyte/macrophages) are critical for the initial inflammatory phase of wound healing and play a key role in the orchestration of subsequent phases.[13,21–23] Blood monocytes originate from macrophage–dendritic cell (DC) precursors in the bone marrow and ultimately differentiate into macrophages and

Received on: September 6, 2017; final version accepted on: February 16, 2018.

From the Department of Surgery (A.K., A.J., F.M.D., A.D., A.B., A.O., P.K.H., K.A.G.), Department of Pathology (M.S., S.L.K.), Department of Pediatrics (J.B.), and Department of Microbiology and Immunology (B.M.), University of Michigan, Ann Arbor.

The online-only Data Supplement is available with this article at http://atvb.ahajournals.org/lookup/suppl/doi:10.1161/ATVBAHA.118.310703/-/DC1.

Correspondence to Katherine A. Gallagher, MD, Department of Surgery, University of Michigan, 1500 E Medical Center Dr, SPC 5867, Ann Arbor, MI 48109-5867. E-mail kgallag@med.umich.edu

Nonstandard Abbreviations and Acronyms	
DC	dendritic cell
DIO	diet-induced obese
FACS	fluorescent activated cell sorting
IL	interleukin
RNA-seq	RNA-sequencing
TGF	transforming growth factor
TNF	tumor necrosis factor

DCs in the tissues.[22,24,25] Given the shared origin between these more differentiated cell progeny, there has been considerable debate about the definitions of these separate cell populations because they retain many of the same surface markers and display overlapping functions.[26] In addition, these definitions are further complicated by the recent discovery of resident macrophages (CD11b$^+$/F4/80$^+$) which populate the tissues before birth and persist through self-replication.[27]Although there is some literature on the role of resident macrophages and DCs in wound healing, there is growing evidence that infiltrating monocyte/macrophages provide the mandatory drive for acute inflammation and subsequently orchestrate the process of repair.[10,14,21,22,28–33] Despite this evidence of the importance of recruited blood monocyte/macrophages, because of lack of consensus definitions and the recent realization that many of the markers previously used to define recruited monocyte/macrophages actually label resident macrophages, few studies have directly examined the in vivo characteristics of the true recruited monocyte/macrophage population. Among blood monocytes, specific identifiable subsets with distinct effector functions have now been identified.[34,35] For instance, Ly6C^{Hi} (Gr1^{Hi}CCR2$^+$CX3CR1^{Lo}) have been shown to promote inflammation, whereas Ly6C^{Lo} (Gr1^{Lo}CCR2$^-$CX3CR1^{Hi}) monocytes are more regenerative.[13,21–23,30–32,34,36] Human correlates for these cells are well described and consist of CD14$^+$CD16$^-$ and CD14$^-$CD16$^+$ monocytes matched with Ly6C^{Hi} and Ly6C^{Lo} murine monocytes, respectively.[13,34,37,38]

Although many in vitro studies using monocyte/macrophages have demonstrated high plasticity, little is known about the wound in vivo cell plasticity.[26] Unfortunately the majority of wound healing literature to date has relied on in vitro definitions of M1 and M2 macrophages, making the application to in vivo studies purely speculative.[7] Although significant strides have been made in recognizing the contribution of blood monocyte-derived macrophages to tissue repair, it remains challenging to study monocyte/macrophage polarity/plasticity in vivo because of a lack of consensus on nomenclature, cell-marker definitions, and debate over effector-cell origin.[7,26] Hence, a careful evaluation of infiltrating monocyte/macrophage subsets in wound granulation tissue is necessary to effectively compare monocyte/macrophage plasticity in both normal and diabetic tissue.

To first define the kinetics of blood monocyte/macrophage subsets in normal and diabetic wound healing, we evaluated Ly6C^{Hi} [Lin$^-$ (CD3$^-$CD19$^-$NK1.1$^-$Ter-119$^-$) Ly6G$^-$CD11b$^+$] (CD11b$^+$Ly6C^{Hi}) and Ly6C^{Lo} [Lin$^-$ (CD3$^-$CD19$^-$NK1.1$^-$Ter-119$^-$) Ly6G$^-$CD11b$^+$] (CD11b$^+$Ly6C^{Lo}) cell influx into murine wound granulation tissue overtime and performed RNA-sequencing (RNA-seq)–based transcriptome profiling of sorted Ly6C^{Hi} and Ly6C^{Lo} cells from both diabetic and nondiabetic murine wounds. We found that during normal healing, CD11b$^+$Ly6C^{Hi} monocyte/macrophages are present within 48 hours of injury and rapidly transition to CD11b$^+$Ly6C^{Lo} monocyte/macrophages. Interestingly, in diabetic wounds, there is a second influx of Ly6C^{Hi} monocyte/macrophages during the reparative phase that persists in the tissue and using adoptive transfer of flow-sorted *tdTomato*-labeled CD11b$^+$Ly6C^{Hi} cells, we found that the Ly6C^{Hi} to Ly6C^{Lo} phenotype transition is delayed in diabetic wounds. Further, the RNA-seq data from wound monocyte/macrophages were compared with established in vitro macrophage definitions, to determine the relevance of this traditional nomenclature to in vivo monocyte/macrophages. Our findings suggest that in normal wounds, CD11b$^+$ Ly6C^{Hi} infiltrating monocyte/macrophages correlate well with the classical in vitro M1[LPS,IFNγ] macrophage definition, in terms of both inflammatory mediator production and consensus gene transcriptome analysis. Additionally, we demonstrate that CD11b$^+$Ly6C^{Hi} and CD11b$^+$Ly6C^{Lo} monocyte/macrophages from diabetic wounds differ significantly in their expression of proinflammatory and profibrotic genes when compared with wild-type controls. Finally, we identify that selective modulation of the second CD11b$^+$Ly6C^{Hi} cell influx in diabetic wounds improves wound healing without the adverse effect of global monocyte depletion. These findings extend mechanistic insight into the dynamic functions of monocyte-derived macrophages during both normal and diabetic tissue repair.

Materials and Methods

The data that support the findings of this study are available from the corresponding author on reasonable request. Details for major experimental resources can be found in Table I in the online-only Data Supplement.

Mice

Male C57BL/6 mice (Jackson Laboratory, Bar Harbor, ME) were maintained in breeding pairs at the University of Michigan Unit for Laboratory and Animal Medicine. Male offspring were maintained on a standard normal rodent diet (13.5% kcal saturated fat, 28.5% protein, 58% carbohydrate; Lab Diet) or standard high-fat diet (60% kcal saturated fat, 20% protein, 20% carbohydrate; Research Diets, Inc) for 12 weeks to induce the diet-induced obese (DIO) model of type 2 diabetes mellitus as previously described.[39] Only male C57BL/6 mice develop obesity/glucose intolerance on high-fat diet, thus females cannot be used as a model of obesity/insulin resistance.[39] mT/mG mice (*Gt(ROSA)26Sor*$^{tm4(ACTB-tdTomato,-EGFP)Luo/J}$) were purchased from Jackson Laboratory. Number of mice used per experiment can be found in the figure legend of each corresponding experiment. All animals underwent procedures at 20 to 32 weeks of age with Institutional Animal Care and Use Committee approval.

Wound Model

Mice were anesthetized, dorsal fur was removed with Veet hair removal cream, and the skin was cleaned with sterile water. Full thickness 4-mm punch biopsies were used to create wounds on the midback as described previously.[12]

Assessment of Wound Healing

Wound healing was monitored daily using digital photography with an 8MP iPad camera as described previously.[10] Wound areas were

calculated using an internal scale and National Institutes of Health ImageJ software. Images were evaluated by 2 independent observers.

Wound Cell Isolation

Wounds were harvested with a 6 mm punch biopsy to afford a 1 to 2 mm margin. Wounds were chopped, digested with Liberase TL (Sigma-Aldrich; Cat No. 5401020001)/DNase I (Sigma-Aldrich; Cat No. 9003-98-9) and plunged through a 100 μm nylon filter to yield a single cell suspension.

Ex Vivo Stimulation

Wound cell isolates were plated in Teflon wells and stimulated with LPS (100 ng/mL). After 1 hour, GolgiStop (BD Biosciences; Cat No. 51-2092KZ; 1:2000 dilution) was added and cells were prepared for surface staining.

Magnetic-Activated Cell Sorting

Wounds were digested as described above. Single cell suspensions were incubated with fluorescein isothiocyanate-labeled anti-CD3, anti-CD19, and anti-Ly6G (Biolegend) followed by anti-fluorescein isothiocyanate microbeads (Miltenyi Biotec; Cat No. 130-042-401, 130-049-601). Flow through was incubated with anti-CD11b microbeads (Miltenyi Biotec; Cat No. 130-049-601) to isolate non-neutrophil, non-T cell, non-B cell, and $CD11b^+$ cells.

Flow Cytometry/Fluorescent Activated Cell Sorting

For surface staining, wound cell isolates were collected either directly from wounds or after ex vivo stimulation. Peripheral blood was collected and after red cell lysis and Ficoll separation, cells were processed for surface staining. Cells were stained with a Fixable LIVE/DEAD viability dye (Molecular Probes by Life Technologies; Ref No. L34959; 1:1000 dilution). FcR-receptors were then blocked with anti-CD16/32 (BioXCell, Cat No. CUS-HB-197, 1:200 dilution) for 10 minutes. Monoclonal antibodies for surface staining included: Anti-CD3 (Biolegend, Cat No. 100304, 1:400 dilution), Anti-CD19 (Biolegend, Cat No. 115504, 1:400 dilution), Anti-Ter-119 (Biolegend, Cat No. 116204, 1:400 dilution), Anti-NK1.1 (Cat No. 108704, 1:400 dilution), Anti-Ly6G (Biolegend, Cat No. 127604, 1:400 dilution), Anti-CD11b (Biolegend, Cat No. 101230, 1:400 dilution), Anti-Ly6C (Biolegend, Cat No. 128035, 1:400 dilution) and Anti-F4/80 (Biolegend, Cat No. 123121, 1:400 dilution). After surface staining, cells were washed twice, and biotinylated antibodies were labeled with streptavidin-fluorophore (Biolegend, Cat No. 405208, 1:1000 dilution). Next, cells were either washed and acquired for surface-only flow cytometry or were fixed with 2% formaldehyde and then washed/permeabilized with BD Perm/wash buffer (BD Biosciences, Ref No. 00-8333-56) for intracellular flow cytometry. After permeabilization, intracellular stains included: anti-IL-1β-Pro-PE Cy7 (eBioscience, Ref No. 25-7114-82, 1:200 dilution) and anti-tumor necrosis factor (TNF)-α-APC (Biolegend, Cat No. 506308, 1:200 dilution). Samples were acquired on a 3-Laser Novocyte Flow Cytometer (Acea Biosciences) or fluorescent activated cell sorting (FACS) sorted on a FACsAria III Flow Sorter. FACS was performed with FACsDiva Software (BD Biosciences), analysis was performed using FlowJo software version 10.0 (Tree Star), and data were compiled using Prism software (GraphPad). All populations were routinely backgated to verify gating and purity. $CD11b^+Ly6C^{Hi}$ and $CD11b^+Ly6C^{Lo}$ monocyte/macrophages were sorted for RNA-seq and adoptive transfer experiments.

RNA-Sequencing

Two biological replicates from normal rodent diet and high-fat diet mice were surface stained and sorted by FACS into $CD11b^+Ly6C^{Hi}$ and $CD11b^+Ly6C^{Lo}$ populations. RNA isolation was performed using a miRNeasy Micro Kit (Qiagen) with DNAse digestion. Because of low RNA yields, library construction was performed using the Clontech SMARTer Pico Kit (Mountain View, CA). Resulting reads were trimmed using Trimmomatic and mapped using HiSAT2.[40,41] Read counts were performed using the feature-counts option from the subRead package followed by the elimination of low reads, normalization, and differential gene expression using edgeR.[42,43] For comparison to in vitro macrophages, an M1[IFNγ] data set from transcriptome data by Piccolo et al[44] and an M1[LPS,IFNγ] and M2[IL-4] data set by Jha et al[45] were used. All reads were mapped to the mm^{10} genome. Differential expression was performed on mapped reads using the tagwise dispersion algorithm in edgeR.[43,46]

Adoptive Transfer

Blood leukocytes from mT/mG mice were passed through a Ficoll gradient and the buffy coat was collected. The mononuclear cell suspension was washed in magnetic-activated cell sorting buffer, labeled with anti-CD3-Biotin, anti-CD19-Biotin, anti-NK1.1-Biotin antibodies (Biolegend), and ultimately, anti-biotin micromagnetic beads (Miltenyi Biotec). The cells were then passed through a magnetic-activated cell sorting column for negative selection. Cells were then surface stained and FACS sorted (as described) to obtain a pure $Ly6C^{Hi}$ population. Approximately 24 hours after wounding, $\approx 10^6$ $tdtomato^+$ $Ly6C^{Hi}$ blood monocytes were injected via tail vein into control and DIO mice. Wounds and peripheral blood were then collected on day 4 postinjury for flow analysis.

MCP-1 Assay

Wound cells were analyzed for MCP-1 (monocyte chemoattractant protein-1) levels using DuoSt ELISA kit (R&D Systems; Cat No. SMJE00) according to the manufacturer's protocol.

RNA Extraction

Total RNA extraction was performed with Trizol using the manufacturer instructions. Total RNA was reverse transcribed to cDNA using iScript (Biorad). qPCR was performed with 2X Taqman PCR mix using the 7500 Real-Time PCR system. Primers for MCP-1 were purchased from Applied Biosciences. Fold expression was calculated by normalizing to control 18s ribosomal RNA using ($2^{\Delta Ct}$) analysis. All samples were assayed in triplicate.

Statistical Analysis

GraphPad Prism software version 6.0 was used to analyze the data. Data are presented as the mean±SEM. Data were first analyzed for normal distribution and then statistical significance between multiple groups was determined using 1-way analysis of variance followed by Newman–Keuls post hoc test. For all other single group comparisons, if data passed normality test, we used 2-tailed Student *t* test. Otherwise, data were analyzed using Mann–Whitney *U* test. All data are representative of at least 2 independent experiments. A P value of ≤ 0.05 was significant.

Results

$CD11b^+Ly6C^{Hi}$ Monocyte/Macrophages Rapidly Accumulate After Skin Injury and Transition to $CD11b^+Ly6C^{Lo}$ Macrophages

Monocyte/macrophages are highly plastic in their roles in acute inflammation, and hence, possess dichotomous roles in both tissue destruction and tissue repair after injury.[23,32] Given the opposing effector functions of distinct cell subsets, a high degree of regulation is necessary for proper repair of injured tissue.[19] Indeed, there is a growing body of evidence that suggests infiltrating monocyte/macrophages contribute significantly to inflammatory conditions, including diabetes mellitus, because of an imbalance of pro- and anti-inflammatory monocyte/macrophages.[8,10,12,23,30] Although this is widely accepted, the

kinetics of myeloid subset influx in wound healing overtime has remained elusive. Because the kinetics of recruited monocyte/macrophage subsets Ly6C^{Hi} (Gr1^{Hi}CCR2^{+}CX3CR1^{Lo}) and Ly6C^{Lo} (Gr1^{Lo}CCR2^{-}CX3CR1^{Hi}) after injury in normal wounds has not been well-defined, wounds from C57BL/6 mice were collected daily postinjury and processed for flow cytometry. Our outlined gating strategy removed doublets, nonviable cells, and neutrophils (Ly6G^{-}), selecting CD11b^{+} cells. Proportions of CD11b^{+}Ly6C^{Hi} and CD11b^{+}Ly6C^{Lo} cells were determined as shown in the density plot (Figure 1A). There is a clearly identifiable CD11b^{+}Ly6C^{Hi} and CD11b^{+}Ly6C^{Lo} population at each time point in the wounds, consistent with data from other organs (Figure 1B).[23] The relative proportions of the CD11b^{+}Ly6C^{Hi} and CD11b^{+}Ly6C^{Lo} cells in wounds change overtime. For the first 24 to 48 hours there is a 4-fold predominance in CD11b^{+}Ly6C^{Hi} monocyte/macrophages in the wounds (≈80:20 at 24 hours), however, eventually the CD11b^{+}Ly6C^{Lo} cohort dominates around 48 hours (Figure 1C). To confirm our focus on infiltrating monocyte/macrophages and not resident macrophages (CD11b^{+}/F4/80^{+}), we examined resident tissue macrophages in our wound granulation tissue and found that they were a small percentage of cells that did not influence our CD11b^{+}Ly6C^{Hi} cells in wounds (Figure I in the online-only Data Supplement). In addition to the changes in myeloid cell subsets in wounds overtime, these findings demonstrate the ability to track and compare 2 independent monocyte/macrophage populations in wounds.

Wound CD11b^{+}Ly6C^{Hi} and CD11b^{+}Ly6C^{Lo} Monocyte/Macrophages Reveal Distinct Inflammatory Profiles

It has been previously shown in other tissues that Ly6C^{Hi} monocyte/macrophages display an inflammatory phenotype. To evaluate whether CD11b^{+}Ly6C^{Hi} monocyte/macrophages in wounds are proinflammatory with respect to their CD11b^{+}Ly6C^{Lo} counterparts, wounds were collected on day 2 postinjury. After ex vivo stimulation, wounds were analyzed by flow cytometry after gating out doublets, nonviable cells, lineage cells [CD3, CD19, NK1.1, Ter-119]$^{-}$, and neutrophils [Ly6G]$^{-}$. The resultant population was then selected for CD11b^{+} cells and then Ly6C^{Hi} or Ly6C^{Lo} monocyte/macrophages (Figure 2A). Selectively, percentages and mean fluorescence intensity (MFI) of TNF-α and IL (interleukin)-1β–producing cells were calculated from the Ly6C^{Hi} and Ly6C^{Lo} populations (Figure 2B). An FMO (fluorescence minus one) control was used to verify the accuracy of gate placement (Figure 2C). Significantly more CD11b^{+}Ly6C^{Hi} monocyte/macrophages were proinflammatory when compared with CD11b^{+}Ly6C^{Lo} monocyte/macrophages. Specifically, CD11b^{+}Ly6C^{Hi} monocyte/macrophages had 27.7% positive cells for IL-1β and 28.5% positive cells for TNF-α; compared with 9.1% and 13.7% in CD11b^{+}Ly6C^{Lo} cells, respectively. Comparably, the MFI of IL-1β and TNF-α were 1457 and 4060 in CD11b^{+}Ly6C^{Hi} versus 524 and 2025 in CD11b^{+}Ly6C^{Lo} cells, respectively. Based on this data, these 2 monocyte/macrophage subsets display different phenotypes in wounds with respect to inflammation. Interestingly, when we examined CD11b^{+}Ly6C^{Hi} and CD11b^{+}Ly6C^{Lo} wound cells for transforming growth factor (TGF)-β, an M2-like cytokine involved in tissue repair, we found that CD11b^{+}Ly6C^{Lo} cells produced significantly more TGF-β compared with wound CD11b^{+}Ly6C^{Hi} cells (Figure II in the online-only Data Supplement). These findings suggest that Ly6C^{Hi} and Ly6C^{Lo} subsets play distinctly different roles in tissue repair and quantification of their proportions may be useful in pathological settings for prognostication and to identify therapeutic targets.

Diabetic Wounds Demonstrate a Second, Late Influx of CD11b^{+}Ly6C^{Hi} Monocyte/Macrophages

Given the differences in inflammatory cytokine production between Ly6C monocyte/macrophage subsets in normal wounds, we hypothesized that excess CD11b^{+}Ly6C^{Hi} cells and decreased CD11b^{+}Ly6C^{Lo} cells could contribute to the pathological inflammation seen in diabetes mellitus.[10,19] To address this, a physiological murine model of type 2 diabetes mellitus (DIO; 60% saturated fat diet) was used. The DIO model was used as opposed to other models of type 2 diabetes mellitus because of its lack of alterations in the innate immune system.[47–49] Similar to normal control mice (Figure 1B and 1C), the DIO wounds demonstrated an early influx of CD11b^{+}Ly6C^{Hi} monocyte/macrophages that transitioned to CD11b^{+}Ly6C^{Lo} monocyte/macrophage dominance around 48 hours. However, in the DIO wounds, there was a second influx of CD11b^{+}Ly6C^{Hi} monocyte/macrophages between days 3 and 4 postinjury that persisted until day 7 (Figure 3A). Furthermore, when comparing percentages of CD11b^{+}Ly6C^{Hi} monocyte/macrophages postinjury between control and DIO mice, at day 4, CD11b^{+}Ly6C^{Hi} monocyte/macrophages represented 22.2% in control mice and 54.3% in DIO mice (Figure 3B). There were no changes in overall CD11b^{+} wound cell numbers or F4/80^{+} resident macrophages between the DIO and control groups, suggesting that the proportional shift in Ly6C populations drives inflammation in the tissue (Figures III and IV in the online-only Data Supplement). Additionally, although there is an increase in the proportion of CD11b^{+}Ly6C^{Hi} cells in DIO wounds, there is a reciprocal decrease in the percentages of CD11b^{+}Ly6C^{Lo} cells in DIO wounds compared with controls (Figure V in the online-only Data Supplement). The predominance of CD11b^{+}Ly6C^{Hi} monocyte/macrophages in DIO wounds at late time points is consistent with previously published data demonstrating increased inflammatory macrophages in diabetic wounds.[8,10,12] To evaluate whether the second influx of CD11b^{+}Ly6C^{Hi} monocyte/macrophages retain their proinflammatory phenotype in late DIO wounds, we performed intracellular flow cytometry for TNF-α and IL-1β. CD11b^{+}Ly6C^{Hi} monocyte/macrophages were 41.2% and 40.2% positive for IL-1β and TNF-α, whereas CD11b^{+}Ly6C^{Lo} monocyte/macrophages were 9.4% and 18.4% positive, respectively. In parallel, the MFI of IL-1β and TNF-α in the Ly6C^{Hi} gate was significantly increased compared with the Ly6C^{Lo} gate (Figure 3C). To compare changes in wound Ly6C populations with changes in CD11b^{+}Ly6C^{Hi} cells in peripheral blood, we analyzed blood CD11b^{+}Ly6C^{Hi} cell proportions in injured and uninjured mice, as well as in control and DIO mice (Figure VI in the online-only Data Supplement). Interestingly, similar to what was demonstrated

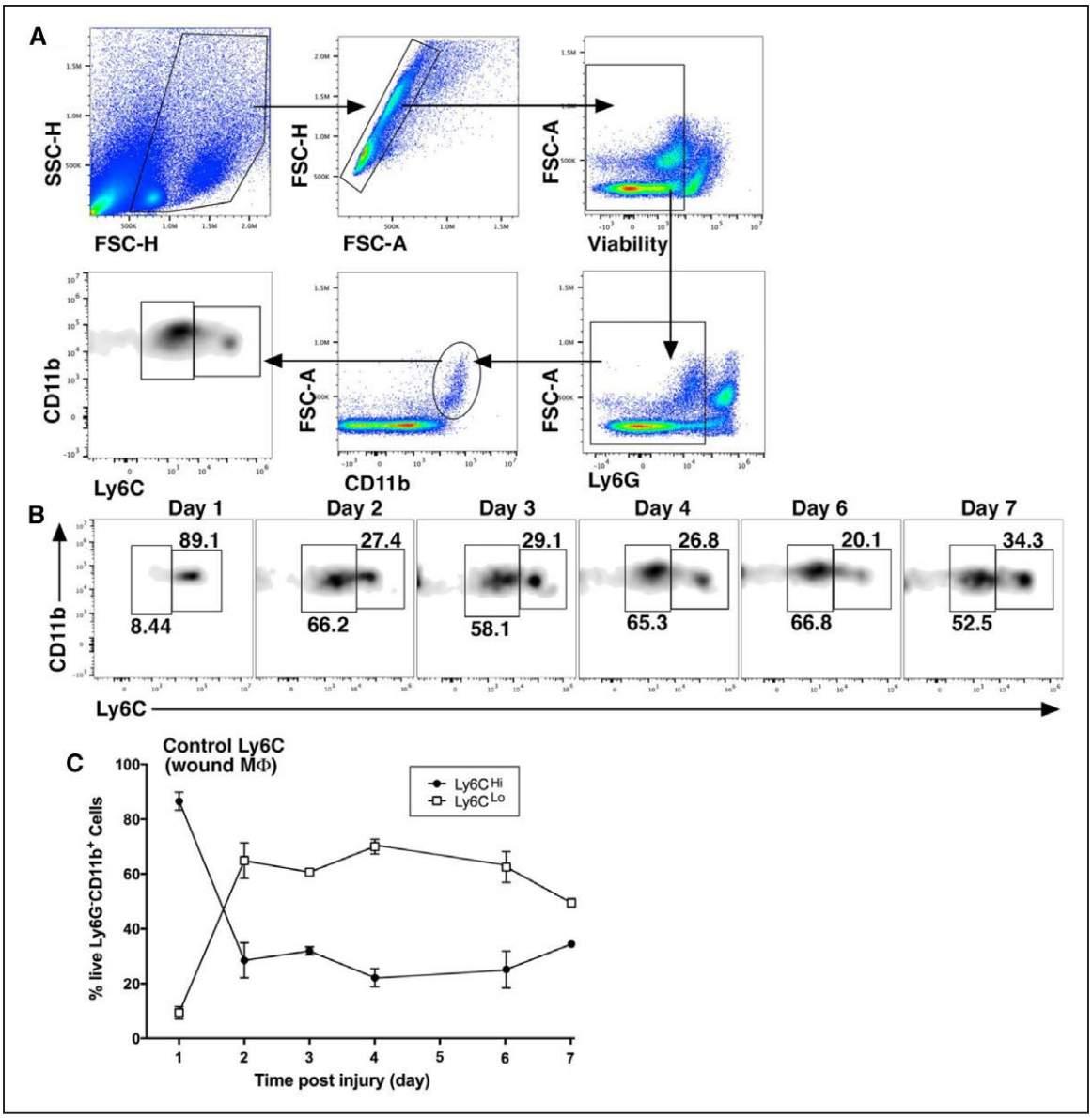

Figure 1. Ly6C^{Hi} [Live, Ly6G^{-}, CD11b^{+}] monocyte/macrophages rapidly accumulate during the first 24 to 48 h after injury and then transition to Ly6C^{Lo} [Live, Ly6G^{-}, CD11b^{+}] cells. Wounds were created using a 4-mm punch biopsy on the back of male C57BL/6 mice. Wounds were harvested daily for 7 d postinjury and analyzed by flow cytometry. **A**, Gating strategy to select single, live, Ly6G^{-}, CD11b^{+} cells and stratify by Ly6C^{Hi} vs Ly6C^{Lo}. **B**, Representative flow plots of Ly6C^{Hi} [Live, Ly6G^{-}, CD11b^{+}] and Ly6C^{Lo} [Live, Ly6G^{-}, CD11b^{+}] cells on postinjury days 1 to 7. **C**, Ly6C^{Hi} [Live, Ly6G^{-}, CD11b^{+}] and Ly6C^{Lo} [Live, Ly6G^{-}, CD11b^{+}] cells plotted as a percentage of CD11b^{+} cells (n=32 mice; tissues of 2 wounds per mouse were pooled for a single biological replicate. Data are representative of 3 independent experiments). All data are expressed as the mean±SEM.

by Swirski et al,[50] we found that there is an increase in peripheral blood CD11b^{+}Ly6C^{Hi} cells after injury. Further, when we looked at differences in peripheral blood CD11b^{+}Ly6C^{Hi} cells between wounded control and DIO mice, there were significantly less CD11b^{+}Ly6C^{Hi} cells in DIO peripheral blood at day 4 postinjury. This suggests that these blood cells may be rapidly recruited to the site of injury in DIO mice and result in an inverse relationship in CD11b^{+}Ly6C^{Hi} cell numbers in peripheral blood and wound tissue. Taken together, these findings suggest that the increased inflammatory phenotype seen in diabetic wounds is secondary to increased CD11b^{+}Ly6C^{Hi} blood monocyte/macrophages and decreased CD11b^{+}Ly6C^{Lo} monocyte/macrophages at late time points after injury.

Diabetic Wound CD11b^{+}Ly6C^{Hi} Cells Display an Impaired Transition to the CD11b^{+}Ly6C^{Lo} Phenotype

CD11b^{+}Ly6C^{Hi} monocyte/macrophages have been shown in other tissues to mature to a less inflammatory CD11b^{+}Ly6C^{Lo} phenotype,[31,51] however, in wound tissue and particularly diabetic wounds, this has not been evaluated. Hence, another potential mechanism of CD11b^{+}Ly6C^{Hi} predominance in DIO wounds may be a failure of CD11b^{+}Ly6C^{Hi} monocyte/macrophages to differentiate to the less inflammatory CD11b^{+}Ly6C^{Lo} cells. To confirm that CD11b^{+}Ly6C^{Hi} cells are recruited to the wound from peripheral blood and to evaluate their progression in wounds from a CD11b^{+}Ly6C^{Hi} to a CD11b^{+}Ly6C^{Lo}

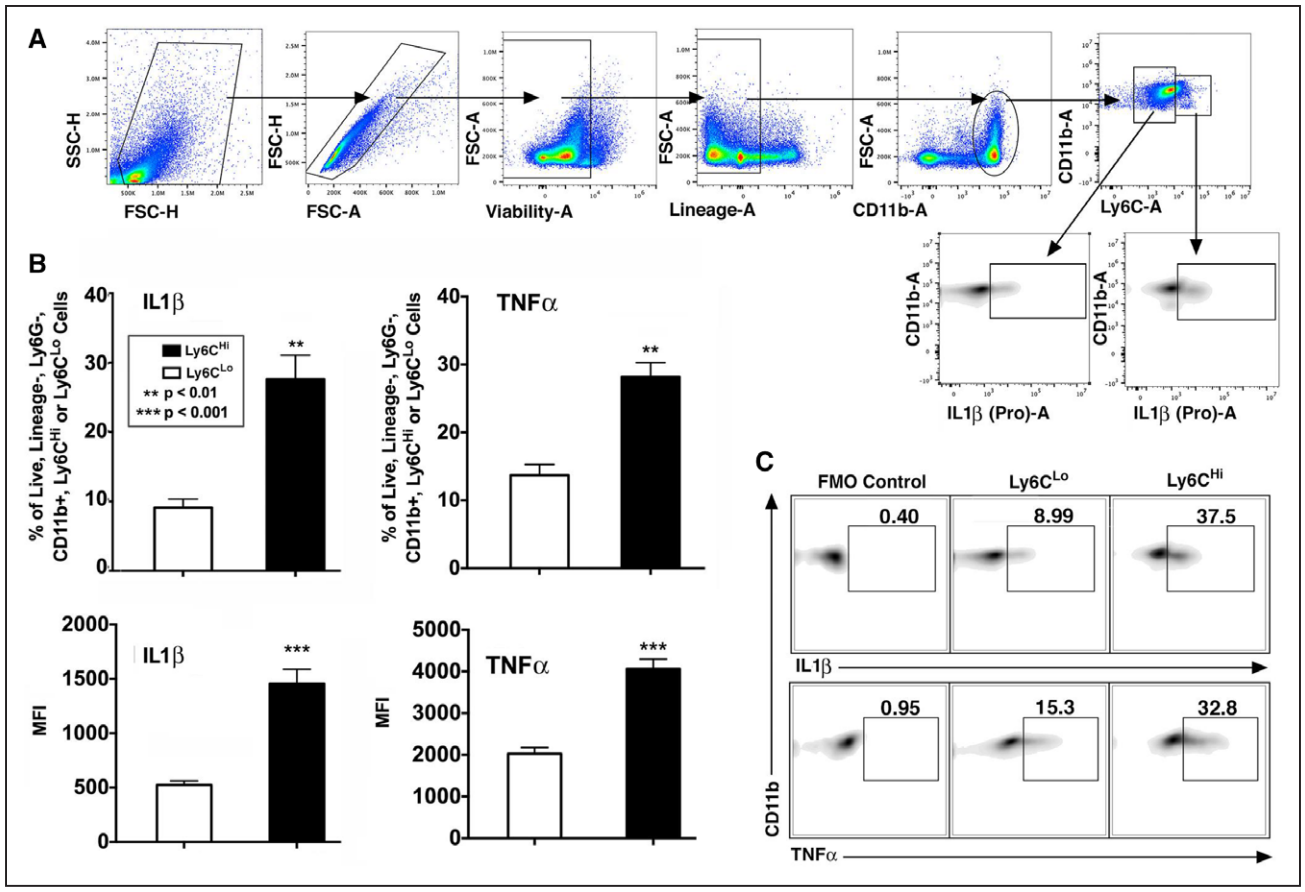

Figure 2. Wound CD11b^{+}Ly6C^{Hi} and CD11b^{+}Ly6C^{Lo} monocyte/macrophages display distinct inflammatory profiles. Wounds from C57BL/6 mice were collected on postinjury day 2 for cell isolation, ex vivo stimulation, and intracellular staining for flow cytometry. **A**, Gating strategy to select single, live, lineage^{-} [CD3, CD19, NK1.1, Ter-119]$^{-}$, Ly6G^{-}, CD11b^{+}, Ly6C^{Hi}, and Ly6C^{Lo} cells. **B**, **Top**, Percentage (%) of Ly6C^{Hi} vs Ly6C^{Lo} cells staining positive for IL (interleukin)-1β and tumor necrosis factor (TNF)-α. **Bottom**, Mean fluorescence intensity (MFI) of IL-1β and TNF-α in the Ly6C^{Hi} and Ly6C^{Lo} gate (**P<0.01, ***P<0.001; n=10 mice; tissues of 2 wounds per mouse were pooled for a single biological replicate. Data are representative of 3 independent experiments). **C**, Representative density plots of Ly6C^{Hi} and Ly6C^{Lo} cells stratified for IL-1β and TNF-α with FMO (fluorescence minus one) control. All data are expressed as mean±SEM.

phenotype, we performed a series of adoptive transfer experiments. Specifically, control and DIO mice were wounded at time zero and ≈24 hours later underwent adoptive transfer with 10^6 CD11b^{+}Ly6C^{Hi} blood monocytes harvested from mT/mG mice (*Gt(ROSA)26Sor$^{tm4(ACTB-tdTomato,-EGFP)Luo}$*/J). Wounds were harvested on day 4 (gating strategy identical to Figure 2A) and flow analysis was performed on the samples by first selecting tdTomato^{+} [Lin^{-}Ly6G^{-}CD11b^{+}] cells and then stratifying by Ly6C to identify the adoptively transferred CD11b^{+}Ly6C^{Hi} monocyte/macrophages (Figure 4A). Adoptively transferred tdTomato^{+} CD11b^{+}Ly6C^{Hi} cells were detectable in the wounds of both control and DIO mice after 3 days. Further, as described previously,[31,51] adoptively transferred CD11b^{+}Ly6C^{Hi} monocyte/macrophages make a transition to a CD11b^{+}Ly6C^{Lo} phenotype, however, this transition seems to be impaired in DIO wounds. Importantly, we observed an approximate 70:30 proportion of Ly6C^{Hi} to Ly6C^{Lo} monocyte/macrophages in DIO mice compared with an approximate 50:50 proportion in control mice (Figure 4B). Taken together, these findings suggest that the proinflammatory CD11b^{+}Ly6C^{Hi} monocyte/macrophage predominance in DIO wounds is related to both an increased recruitment and impaired differentiation of CD11b^{+}Ly6C^{Hi} cells in a diabetic setting.

Diabetic Wound CD11b^{+}Ly6C^{Hi} and CD11b^{+}Ly6C^{Lo} Cells Reveal Distinct Transcriptome Profiles

Literature examining the hyperinflammatory state of diabetic wounds has drawn loose comparisons between in vivo wound monocyte/macrophages and classical or alternative in vitro macrophages.[5,8–10] Although this can be helpful for descriptive purposes, it is hindered by inconsistencies in nomenclature and a degree of overlap in in vivo wound monocyte/macrophage subsets that do not fit discrete in vitro definitions.[7,21] Further, to our knowledge, the comparison of diabetic and control wound monocyte/macrophages with in vitro M1[LPS/IFNγ], M1[IFNγ], or M2[IL-4] macrophages has not been examined using whole transcriptome profiling. Because the gene expression profiles of in vivo Ly6C^{Hi} [Lin^{-}Ly6G^{-}CD11b^{+}] and Ly6C^{Lo} [Lin^{-}Ly6G^{-}CD11b^{+}] monocyte/macrophage populations in wounds are unknown because of the lack of transcriptome data, we first sought to evaluate by RNA-seq, if in vivo infiltrating Ly6C^{Hi} [Lin^{-}Ly6G^{-}CD11b^{+}] and Ly6C^{Lo} [Lin^{-}Ly6G^{-}CD11b^{+}] monocyte/macrophages from DIO and normal wounds correlate with traditional definitions of in vitro M1[LPS,IFNγ] or M2[IL-4] macrophages.[7] Single cell suspensions from control and DIO wounds (2 biological replicates/group; 4 mice/replicate) were washed, surface stained,

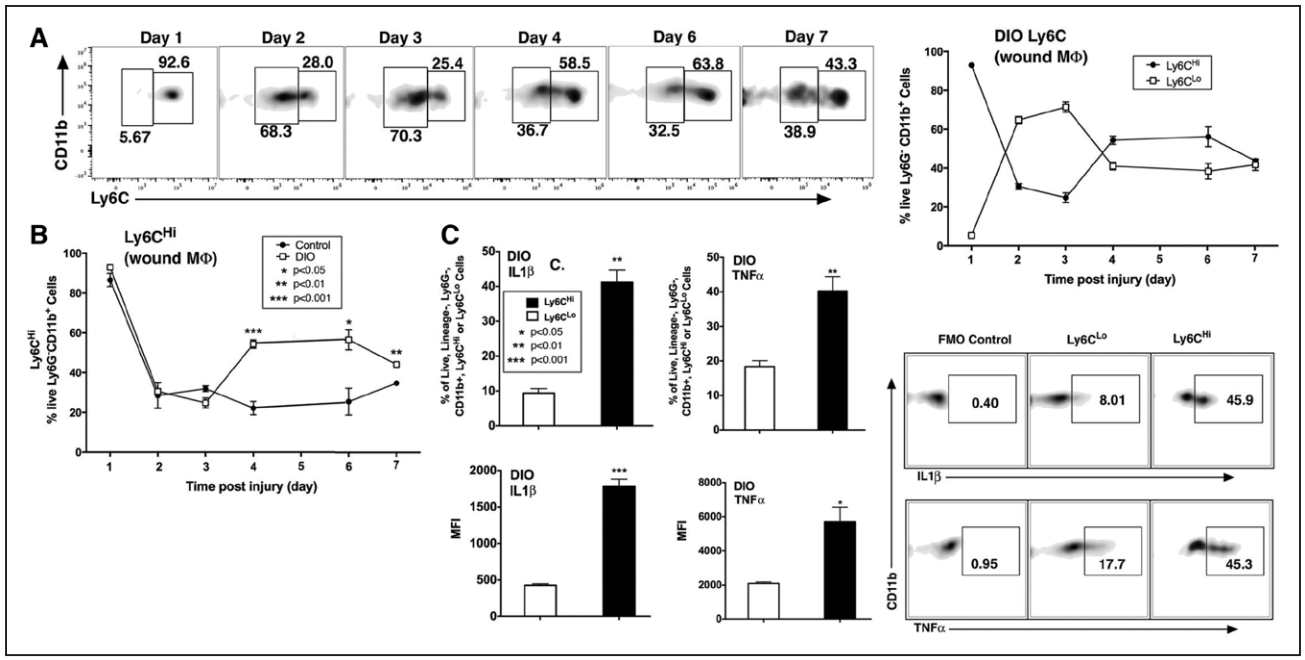

Figure 3. Diabetic wounds demonstrate a second, late influx of CD11b$^+$Ly6C^{Hi} monocyte/macrophages. C57BL/6 mice were fed high fat (HFD) chow (60% kCal) for 12 to 16 wk to induce obesity and insulin resistance/glucose intolerance in the diet-induced obese model (DIO) of physiological type 2 diabetes mellitus. Wounds were collected on postinjury days 1 to 7 for flow cytometry. **A**, Representative density plots of DIO Ly6C^{Hi} [Live, Ly6G$^-$, CD11b$^+$] and DIO Ly6C^{Lo} [Live, Ly6G$^-$, CD11b$^+$] cells on postinjury days 1 to 7. Gating strategy was identical to Figure 1. DIO Ly6C^{Hi} [Live, Ly6G$^-$, CD11b$^+$] and DIO Ly6C^{Lo} [Live, Ly6G$^-$, CD11b$^+$] cells plotted as a percentage of CD11b$^+$ cells (n=32 mice; tissues of 2 wounds per mouse were pooled for a single biological replicate. Data are representative of 3 independent experiments). **B**, Direct comparison of control and DIO Ly6C^{Hi} [Live, Ly6G$^-$, CD11b$^+$] cells overtime after injury. (*P<0.05, **P<0.01, ***P<0.001; n=4 mice per group per time point; tissues of 2 wounds per mouse were pooled for a single biological replicate. Data are representative of 2 experiments). **C**, DIO wounds were collected on postinjury day 2 for cell isolation, ex vivo stimulation, and intracellular staining for flow cytometry. Representative density plots of DIO Ly6C^{Hi} and Ly6C^{Lo} [Lin$^-$, Ly6G$^-$, CD11b$^+$] cells as gated in Figure 2, stratified for IL-1β and TNF-α. **Top**, % of DIO CD11b$^+$Ly6C^{Hi} vs DIO CD11b$^+$Ly6C^{Lo} cells staining positive for IL-1β and TNF-α. **Bottom**, Mean fluorescence intensity (MFI) of IL-1β and TNF-α in the DIO CD11b$^+$Ly6C^{Hi} and DIO CD11b$^+$Ly6C^{Lo} gate (*P<0.05, **P<0.01, ***P<0.001; n=5 mice/group; tissues of 2 wounds per mouse were pooled for a single biological replicate. Data are representative of 2 experiments).

and FACS sorted into Ly6C^{Hi} [Lin$^-$Ly6G$^-$CD11b$^+$] and Ly6C^{Lo} [Lin$^-$Ly6G$^-$CD11b$^+$] populations. RNA samples were then run by the University of Michigan DNA Sequencing Core. Given that there is dissension in the literature about the definitions of in vitro macrophages, we used the International Congress of Immunology Guidelines (2013) to select gene transcripts for comparison with our wound cells.[7] Specifically, we generated a heat map looking at our wound transcriptome data and compared that directly with publicly available M1[IFNγ], M1[LPS,IFNγ], and M2[IL-4] transcriptome data.[44,45] We first focused on M1 consensus genes: *Arg1, Socs1, Nos2, Marco, Il27, Il23a, Il12a, Il6, Nfkbiz, Tnf, and Irf5* (Figure 5A). Focusing on this specific set of important M1 genes, it is clear that there is a resemblance between in vivo CD11b$^+$Ly6C^{Hi} wound monocyte/macrophages and M1[LPS/IFNγ] in vitro macrophages. Further, when we focused on M2 consensus genes: *Arg1, Chil3, Retnla, Nos2, Ccl24, Marco, Irf4, Ccl22, Ccl17, Alox15, and Socs2*, we found that the genes shared by both subsets, including Arg1 and Nos2, were most strongly expressed by in vivo Ly6C wound monocyte/macrophages (Figure 5B). Many of the genes that were distinct to the M2 subset were not highly expressed by any in vivo subset. Because Ly6C^{Lo} [Lin$^-$Ly6G$^-$CD11b$^+$] monocyte/macrophages represent more of a hybrid picture between in vitro M1 and M2 macrophages, it is possible that the use of traditional in vitro macrophage characterization for this cell population in wound healing is not practical, as has been previously suggested.[21] These findings are highly relevant as they will allow for more accurate immunophenotyping of wound monocyte/macrophages and identify new avenues for therapy. To test the similarity of in vivo monocyte subsets isolated from wounds to traditional in vitro macrophages, we compared the entire transcriptome from each data set (Figure 5C). Figure 5C shows the Pearson correlation for all differentially expressed genes. These data confirm the analysis performed in Figure 5A and 5B and further demonstrate that the in vivo subsets display a distinct profile in comparison to in vitro macrophages.

Because diabetic wounds demonstrate increased recruitment of infiltrating Ly6C^{Hi} [Lin$^-$Ly6G$^-$CD11b$^+$] proinflammatory monocyte/macrophages, we examined whether diabetic CD11b$^+$Ly6C^{Hi} wound cells differ in transcriptome from control wound CD11b$^+$Ly6C^{Hi} monocyte/macrophages. Using edgeR analysis and hierarchical clustering, we found a significant discord between CD11b$^+$Ly6C^{Hi} monocyte/macrophages from control and diabetic wounds. Many of these genes are important in inflammation and collagen formation and are thus, important for wound healing (Table II in the online-only Data Supplement). Taken together, these findings suggest that increased inflammation in diabetic wounds is the result of both an additional late influx of proinflammatory CD11b$^+$Ly6C^{Hi} monocyte/macrophages as well as altered phenotypes of these monocyte/macrophages in the diabetic environment.

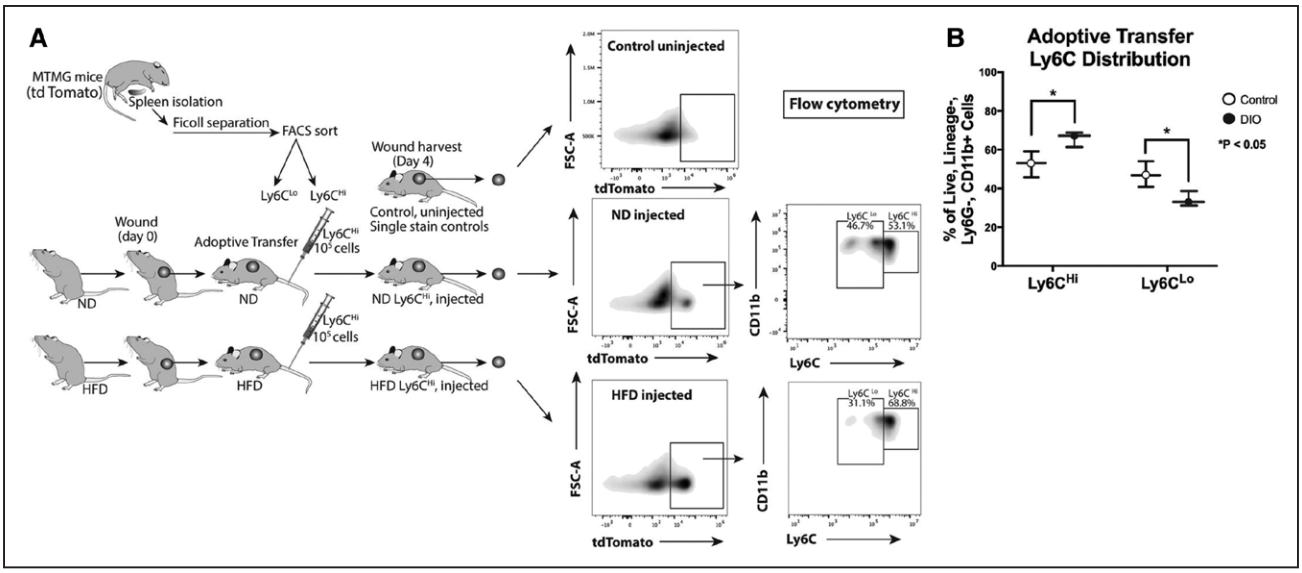

Figure 4. Diabetic wound CD11b$^+$Ly6C^{Hi} cells demonstrate delayed transition to a CD11b$^+$Ly6C^{Lo} phenotype. **A**, Schematic of adoptive transfer experiment in which 10^6 *tdTomato*-expressing Ly6C^{Hi} [Lin$^-$, Ly6G$^-$, CD11b$^+$] peripheral blood cells were injected via tail vein into control and DIO mice 24 h after wounding. Control and DIO wounds were harvested on day 4 (3 d postadoptive transfer) and single cell suspensions were processed for flow cytometry. Representative density plots of adoptively transferred control and DIO wounds gated for tdTomato$^+$ [Lin$^-$Ly6G$^-$CD11b$^+$] cells and then stratifying by Ly6C designation. **B**, Control and DIO wounds were harvested on day 4 (3 d postadoptive transfer) and single cell suspensions were processed for flow cytometry. Relative percentages of adoptively transferred Ly6C^{Hi} [Lin$^-$Ly6G$^-$CD11b$^+$tdTomato$^+$] and Ly6C^{Lo} [Lin$^-$Ly6G$^-$CD11b$^+$tdTomato$^+$] monocyte/macrophages (*P<0.05; n=6 wounds per group, repeated 1X). All data are expressed as the mean±SE.

Timed Treatment of Diabetic Mice With Anti-MCP-1 Antibody Postinjury Restores Normal Healing

To examine the mechanism responsible for increased CD11b$^+$Ly6C^{Hi} monocyte/macrophages in diabetic wounds, we first identified chemotactic factors that may drive increased recruitment of monocytes from peripheral blood. MCP-1 (CCL2 [C-C motif ligand 2]) is the ligand to the monocyte chemokine receptor CCR2 (C-C chemokine receptor type 2) and is necessary for recruitment of blood monocytes to inflamed tissues.[21,34] Hence, we measured levels of MCP-1 in control and DIO wound cells at a time point during the second CD11b$^+$Ly6C^{Hi} influx in diabetic wounds. When we examined CD3$^+$ lymphocytes, CD19$^+$ B cells, Ly6G$^+$ neutrophils, CD4$^+$ T cells, CD11b$^-$ [CD3, CD19, NK1.1, Ly6G]$^-$ cells, and CD11b$^+$ [CD3, CD19, NK1.1, Ly6G]$^-$ myeloid cells from wounds we found that MCP-1 levels were significantly increased in DIO wound CD11b$^+$ [CD3, CD19, NK1.1, Ly6G]$^-$ cells (wound macrophages as previously defined by our group and others) compared with controls on day 5 following injury (Figure 6A; Figure VII in the online-only Data Supplement).[10,12,52,53] This increase in DIO wound MCP-1 at day 5 is accompanied by increased CD11b$^+$Ly6C^{Hi} monocyte/macrophage counts in DIO wounds at day 6 (Figure 6B).

Prior work in murine models of diabetes mellitus has demonstrated impaired wound healing secondary to increased inflammation.[8,10,12] Given that we found a potential mechanism for increased inflammation in diabetic wounds through the excessive recruitment and retention of CD11b$^+$Ly6C^{Hi} inflammatory monocyte/macrophages, we hypothesized that selective, timed depletion of MCP-1 could improve wound healing by blocking the second influx of CD11b$^+$Ly6C^{Hi} inflammatory monocytes/macrophages. DIO and control mice were wounded and on postinjury day 3 (24 hours before the observed second wave of CD11b$^+$Ly6C^{Hi} monocyte/macrophages), injected with either normal rabbit serum or purified rabbit anti-mouse MCP-1 antibody (anti-MCP-1) and wound healing was monitored. Anti-MCP-1 injected DIO mice demonstrated significantly improved wound healing compared with normal rabbit serum-injected controls (Figure 6C). As expected, in control mice, anti-MCP-1 injection did not significantly alter wound healing, although there was a trend toward impaired healing in the anti-MCP-1 injected mice (Figure 6D). This is similar to other studies demonstrating that impairing monocyte recruitment in normal wound healing is detrimental to healing.[21] Further, when wounds were harvested 2 days after anti-MCP-1 injection, there was a clear reduction in the CD11b$^+$Ly6C^{Hi} cells, suggesting that the improved wound healing seen in the DIO mice after anti-MCP-1 injection correlates with reduced CD11b$^+$Ly6C^{Hi} monocyte/macrophages (Figure 6E and 6F). Additionally, when we examined the blood, there was a trend toward decreased CD11b$^+$Ly6C^{Hi} cells and increased CD11b$^+$Ly6C^{Lo} cells in both the normal and DIO blood after anti-MCP-1 injection (Figure VIII in the online-only Data Supplement). These findings suggest that careful and time-dependent antibody-mediated control of monocyte/macrophage influx after injury may represent a novel therapeutic target for impaired diabetic wound healing.

Discussion

Infiltrating peripheral blood monocyte/macrophages are necessary for the maintenance of tissue homeostasis postinjury.[11,15] Monocyte/macrophages are highly plastic in their roles in acute inflammation, and hence, possess dichotomous roles in both tissue destruction and tissue repair after

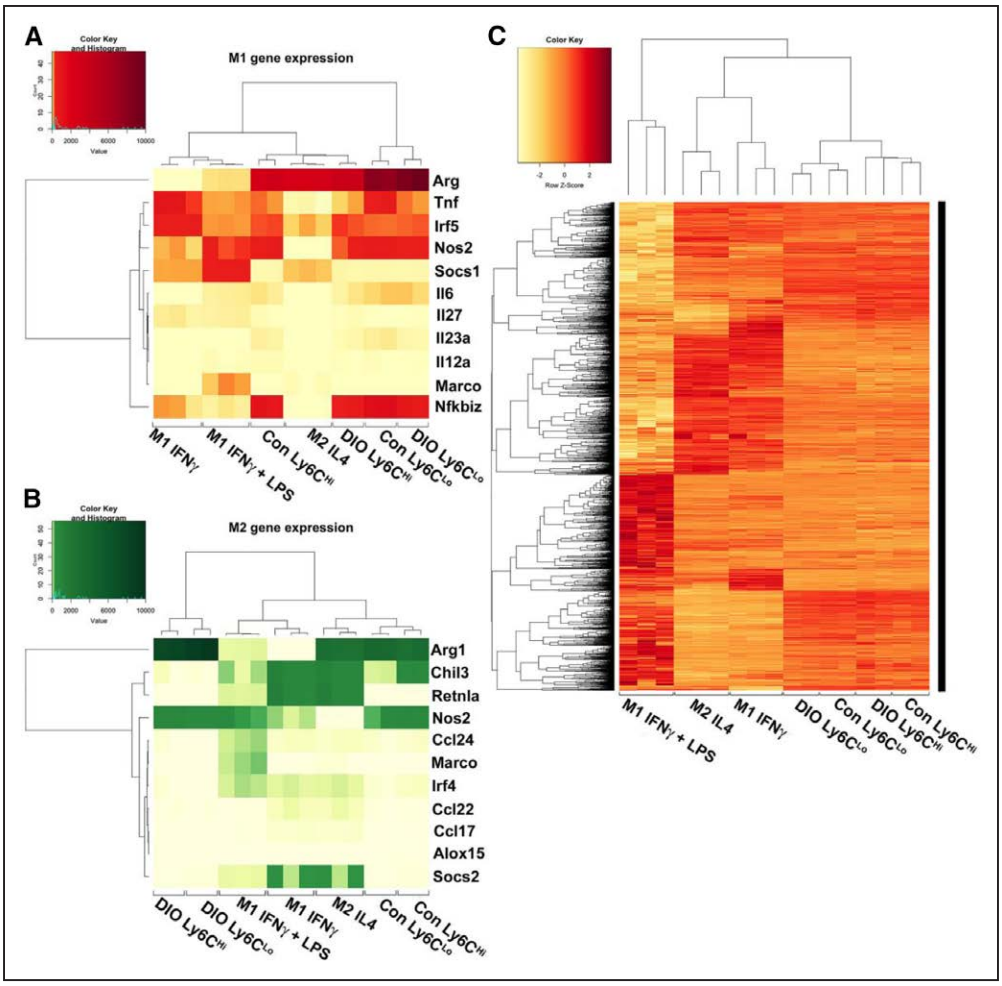

Figure 5. Diabetic wound CD11b$^+$Ly6C^{Hi} and CD11b$^+$Ly6C^{Lo} monocyte/macrophages display distinct transcriptome profiles. Wounds from normal and high-fat diet (HFD)-fed, diet-induced obese (DIO) C57BL/6 mice were collected on postinjury day 3 for cell isolation, surface staining, and fluorescent activated cell sorting (FACS) to isolate Ly6C^{Hi} [Lin$^-$Ly6G$^-$CD11b$^+$] and Ly6C^{Lo} [Lin$^-$Ly6G$^-$CD11b$^+$] monocyte/macrophages for RNA-sequencing (RNA-seq). RNA samples were processed by the National Institutes of Health-funded, University of Michigan DNA sequencing core. Reads were trimmed using Trimmomatic and mapped using HiSAT2. Read counts were performed using the featureCounts option from the subRead package followed by the elimination of low reads and normalization using edgeR. For comparison to in vitro generated macrophages, M1[IFNγ], M1[LPS,IFNγ], and M2[IL-4] data sets were used from publicly available transcriptome data generated by Piccolo et al.[44] **A**, A heatmap of normalized reads obtained from edgeR for an internationally recognized panel of consensus genes for in vitro generated M1 macrophages. Wound Ly6C^{Hi} [Lin$^-$Ly6G$^-$CD11b$^+$] and Ly6C^{Lo}[Lin$^-$Ly6G$^-$CD11b$^+$] monocyte/macrophages were compared with the M1[IFNγ], M1[LPS,IFNγ], and M2[IL-4] transcriptomes. **B**, A heatmap of normalized reads obtained from edgeR for an internationally recognized panel of consensus genes for in vitro generated M2 macrophages. Wound Ly6C^{Hi} [Lin$^-$Ly6G$^-$CD11b$^+$] and Ly6C^{Lo} [Lin$^-$Ly6G$^-$CD11b$^+$] monocyte/macrophages were compared with the M1[IFNγ], M1[LPS,IFNγ], and M2[IL-4] transcriptome. **C**, Clustered Pearson correlation of the entire transcriptome of in vivo DIO and control Ly6C^{Hi} [Lin$^-$Ly6G$^-$CD11b$^+$] and Ly6C^{Lo} [Lin$^-$Ly6G$^-$CD11b$^+$] monocyte/macrophages and in vitro M1[IFNγ], M1[LPS,IFNγ], and M2[IL-4] macrophages (n=8 mice per group; 4 wounds per mouse were pooled to obtain a single biological replicate given low RNA volumes. Two biological replicates per group were examined).

injury.[23,32] Given the opposing effector functions of distinct subsets, a high degree of regulation of these cells is necessary for proper repair of injured tissue.[19] Indeed, there is a growing body of evidence that suggests infiltrating monocyte/macrophages contribute significantly to inflammatory conditions, including diabetes mellitus, because of an imbalance of pro- and anti-inflammatory cells.[8,10,12,23,30] Although this is widely accepted, the kinetics of myeloid cell subset influx in wound healing overtime has remained elusive. Further, the definitions of these cell populations remain elusive, with many previous in vivo cell characterizations based on the inclusion of resident macrophages (CD11b$^+$/F4/80$^+$).[22,26,34] These resident macrophages arise from a separate nonhematopoietic cell lineage, are present at birth and self-renew in the tissues, making them fundamentally distinct from the blood-derived infiltrating monocyte/macrophages that are recruited to tissues after injury.[27,31] Thus, there is little existing literature that examines the phenotype and role of these infiltrating monocyte/macrophages after injury. Hence, we chose a model of wound healing in which we would collect granulation tissue (arguably devoid of resident macrophages; Figure I in the online-only Data Supplement) and our definition Ly6C^{Hi} [Lin$^-$Ly6G$^-$CD11b$^+$] and Ly6C^{Lo} [Lin$^-$Ly6G$^-$CD11b$^+$] as infiltrating monocyte/macrophages based on the previous study that classified these cells with a similar definition.[23,35,52,54,55]

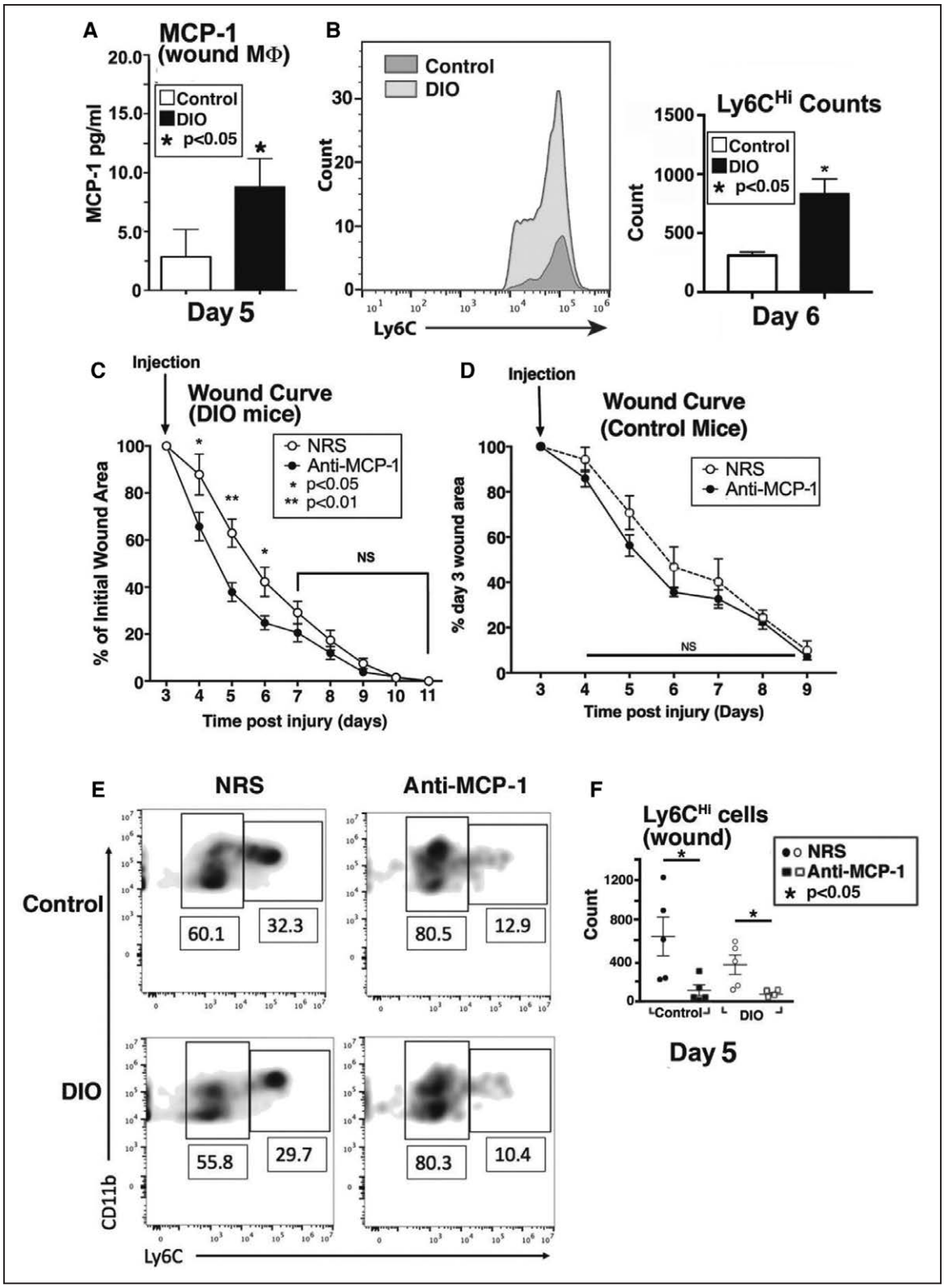

Figure 6. Timed treatment of diabetic mice with anti-MCP-1 (monocyte chemoattractant protein-1) antibody postinjury restores normal healing. **A**, The ligand for the blood monocyte CCR2 (C-C chemokine receptor type 2) receptor, MCP-1, was examined in wound macrophages isolated by magnetic cell sorting CD11b$^+$ [CD3$^-$CD19$^-$NK1.1$^-$Ly6G$^-$] from diet-induced obese (DIO) and control mice on day 5. Protein levels of MCP-1 as determined by ELISA in control and DIO wound cells on day 5 postinjury. (**P<0.05;* n= 5 mice/group; data are representative of 2 independent experiments). **B**, Control and DIO wounds were harvested on day 6 and single cell suspensions were processed for flow cytometry. Ly6C^{Hi} [Live, Ly6G$^-$, CD11b$^+$] monocyte/macrophage counts (as gated in Figure 1) are shown. (**P*<0.05; n=5 mice/group; repeated 1X). **C**, DIO mice were wounded with a 4-mm punch biopsy and wound healing was monitored daily using an 8MP iPad camera, internal scale, and National Institutes of Health (NIH) ImageJ software. At day 3 postinjury, mice underwent intraperitoneal injection with either normal rabbit (*Continued*)

Figure 6 Continued. serum (NRS) or purified rabbit anti-mouse MCP-1 antibody (anti-MCP-1) and wound healing was monitored until wound closure. Wound curves were generated as percent of initial wound area. (*P<0.05, **P<0.01; n=10 wounds per group). **D**, Control mice were wounded with a 4-mm punch biopsy and wound healing was monitored daily using an 8MP iPad camera, internal scale, and NIH ImageJ software. At day 3 postinjury, mice underwent intraperitoneal injection with either normal rabbit serum (NRS) or purified rabbit anti-mouse MCP-1 antibody (anti-MCP-1) and wound healing was monitored until wound closure. Wound curves were generated as percent of initial wound area. (n=10 wounds per group). **E** and **F**, DIO mice were wounded with a 4-mm punch biopsy and on day 3 postinjury, mice underwent intraperitoneal injection with either NRS or purified rabbit anti-mouse MCP-1 antibody (anti-MCP-1). Wounds were harvested on day 5 and analyzed by flow cytometry. Gating was identical to that shown in Figure 2. DIO Ly6C^{Hi} [Lin$^-$Ly6G$^-$CD11b$^+$] and DIO Ly6C^{Lo} [Lin$^-$Ly6G$^-$CD11b$^+$] wound cells from NRS and anti-MCP-1 injected. (*P<0.05; n=25 mice; tissues of 2 wounds per mouse were pooled for a single biological replicate. Data are representative of 2 independent experiments). All data are expressed as mean±SEM.

Herein, we have described the influx of CD11b$^+$Ly6C^{Hi} and CD11b$^+$Ly6C^{Lo} monocyte/macrophages in wound healing in physiological and diabetic conditions, and have found mechanisms for increased inflammation in diabetic wound healing secondary to an increased influx of CD11b$^+$Ly6C^{Hi} cells and a delay in their maturation to CD11b$^+$Ly6C^{Lo} cells. Interestingly, we found an increased number of circulating CD11b$^+$Ly6C^{Hi} monocytes in control wounded mice and when comparing control and DIO wounded mice, there were less circulating CD11b$^+$Ly6C^{Hi} cells in DIO mice although there were more CD11b$^+$Ly6C^{Hi} cells in DIO wounds—suggesting a yin-yang phenomenon in monocyte recruitment in diabetes mellitus. Although this could represent a poor mobilization of splenic and bone marrow-derived monocytes in diabetic mice, it has been demonstrated previously that in the setting of intact CCR2-MCP1 signaling, there is robust mobilization of CD11b$^+$Ly6C^{Hi} monocytes from bone marrow and spleen after injury.[50,56] Additional mechanisms of increased inflammation in diabetic wounds were demonstrated herein using RNA-based transcriptome profiling, where we found that the transcriptome of diabetic wound CD11b$^+$Ly6C^{Hi} and CD11b$^+$Ly6C^{Lo} monocyte/macrophages differs from control cells with respect to proinflammatory and profibrotic gene expression. Importantly, these transcriptome-based studies identify an accurate way to immunophenotype monocyte/macrophages in the wound and may provide a benchmark for response to therapy. Additionally, we have found that a selective, timed injection of anti-MCP-1 antibody resulted in improved wound healing in diabetic mice; suggesting at least a partial amelioration of the impaired wound healing phenotype.

Previous studies have drawn loose comparisons between in vivo wound monocyte/macrophages and classical or alternative in vitro macrophages.[5,8–10] Because it is not clear that in vivo wound monocyte/macrophage subsets fit discrete in vitro definitions,[7,21] we performed a full transcriptome analysis of both diabetic and control wound monocyte/macrophages. Using RNA-seq, we found that the transcriptome of Ly6C^{Hi} [Lin$^-$Ly6G$^-$CD11b$^+$] monocyte/macrophages extracted from normal wounds do resemble in vitro M1[LPS,IFNγ] macrophages. Ly6C^{Lo} [Lin$^-$Ly6G$^-$CD11b$^+$] monocyte/macrophages, however, do not resemble M2 in vitro macrophages. Taken together with our RNA-seq data, this suggests that Ly6C is important in immunophenotyping wound monocyte/macrophages. These findings are highly relevant as they will allow for accurate immunophenotyping and promote caution in drawing comparisons between in vivo wound monocyte/macrophages and traditional in vitro macrophages.

Although this article addresses important issues with regards to the fundamental biology of blood monocyte influx and its relation to wound phenotypes, there are some limitations. First, wound monocyte/macrophages are inextricably related to wound DCs and they are tedious to define with traditional flow cytometry.[22] Thus, it is conceivable that some of our findings are related to wound DCs, however, given the homogenous character of our RNA-seq data between biological replicates, this is unlikely to be relevant. Next, although our RNA-seq comparison of Ly6C^{Hi} [Lin$^-$Ly6G$^-$CD11b$^+$] cells with M1[LPS,IFNγ] data revealed a close resemblance, there are still many differentially expressed genes, which cautions that a direct comparison is still somewhat unreliable except in the confines of comparing consensus genes. Further, although our Ly6C^{Lo} [Lin$^-$Ly6G$^-$CD11b$^+$] RNA-seq data did not show resemblance to the M2[IL-4] transcriptome, our findings of increased TGF-β in CD11b$^+$Ly6C^{Lo} cells is consistent with previously published reports by Olingy et al[57] which found that CD11b$^+$Ly6C^{Lo} cells are predisposed to form CD206$^+$ repair macrophages in wound tissues. Finally, with regard to our translational finding that blocking the MCP-1/CCR2 axis improves late wound healing in diabetes mellitus, the previous study by Willenborg et al[21] suggests that this leukocyte recruitment mechanism is essential for normal wound healing. We agree with this and feel that our findings complement this study, as we found that the timing of MCP-1/CCR2 blockade is important because initial inflammation is critical for proper wound healing.

Our findings herein are both novel and timely, as recent literature has highlighted the importance of blood monocyte/macrophage heterogeneity in health and disease.[35,58] Additional questions remain as to whether blood monocyte chemotaxis modulation or control of monocyte/macrophage phenotype transition will be effective in treating inflammatory conditions. With new research focused on monocyte/macrophage heterogeneity in wounds, it is foreseeable that an improved understanding of chronic inflammatory conditions will lead to new, desperately needed therapeutics.

Acknowledgments

We would like to thank Robin G. Kunkel, Research Associate in the Pathology Department, University of Michigan, for her artistic work.

Sources of Funding

This study was supported by National Institutes of Health (NIH) DK-102357, NIH-T32 HL076123, and the Wolfe Foundation.

Disclosures

None.

References

1. Reiber GE, Vileikyte L, Boyko EJ, del Aguila M, Smith DG, Lavery LA, Boulton AJ. Causal pathways for incident lower-extremity ulcers in patients with diabetes from two settings. *Diabetes Care*. 1999;22:157–162.
2. Faglia E, Favales F, Morabito A. New ulceration, new major amputation, and survival rates in diabetic subjects hospitalized for foot ulceration from 1990 to 1993: a 6.5-year follow-up. *Diabetes Care*. 2001;24:78–83.
3. Dinh T, Tecilazich F, Kafanas A, Doupis J, Gnardellis C, Leal E, Tellechea A, Pradhan L, Lyons TE, Giurini JM, Veves A. Mechanisms involved in the development and healing of diabetic foot ulceration. *Diabetes*. 2012;61:2937–2947. doi: 10.2337/db12-0227.
4. Kannel WB. Risk factors for atherosclerotic cardiovascular outcomes in different arterial territories. *J Cardiovasc Risk*. 1994;1:333–339.
5. Boniakowski AE, Kimball AS, Jacobs BN, Kunkel SL, Gallagher KA. Macrophage-mediated inflammation in normal and diabetic wound healing. *J Immunol*. 2017;199:17–24. doi: 10.4049/jimmunol.1700223.
6. Sica A, Mantovani A. Macrophage plasticity and polarization: in vivo veritas. *J Clin Invest*. 2012;122:787–795. doi: 10.1172/JCI59643.
7. Murray PJ, Allen JE, Biswas SK, et al. Macrophage activation and polarization: nomenclature and experimental guidelines. *Immunity*. 2014;41:14–20. doi: 10.1016/j.immuni.2014.06.008.
8. Mirza RE, Fang MM, Ennis WJ, Koh TJ. Blocking interleukin-1β induces a healing-associated wound macrophage phenotype and improves healing in type 2 diabetes. *Diabetes*. 2013;62:2579–2587. doi: 10.2337/db12-1450.
9. Sindrilaru A, Peters T, Wieschalka S, Baican C, Baican A, Peter H, Hainzl A, Schatz S, Qi Y, Schlecht A, Weiss JM, Wlaschek M, Sunderkötter C, Scharffetter-Kochanek K. An unrestrained proinflammatory M1 macrophage population induced by iron impairs wound healing in humans and mice. *J Clin Invest*. 2011;121:985–997. doi: 10.1172/JCI44490.
10. Gallagher KA, Joshi A, Carson WF, Schaller M, Allen R, Mukerjee S, Kittan N, Feldman EL, Henke PK, Hogaboam C, Burant CF, Kunkel SL. Epigenetic changes in bone marrow progenitor cells influence the inflammatory phenotype and alter wound healing in type 2 diabetes. *Diabetes*. 2015;64:1420–1430. doi: 10.2337/db14-0872.
11. Mantovani A, Biswas SK, Galdiero MR, Sica A, Locati M. Macrophage plasticity and polarization in tissue repair and remodelling. *J Pathol*. 2013;229:176–185. doi: 10.1002/path.4133.
12. Kimball AS, Joshi AD, Boniakowski AE, Schaller M, Chung J, Allen R, Bermick J, Carson WF IV, Henke PK, Maillard I, Kunkel SL, Gallagher KA. Notch regulates macrophage-mediated inflammation in diabetic wound healing. *Front Immunol*. 2017;8:635. doi: 10.3389/fimmu.2017.00635.
13. Italiani P, Boraschi D. From monocytes to M1/M2 macrophages: phenotypical vs. functional differentiation. *Front Immunol*. 2014;5:514. doi: 10.3389/fimmu.2014.00514.
14. Wynn TA, Vannella KM. Macrophages in tissue repair, regeneration, and fibrosis. *Immunity*. 2016;44:450–462. doi: 10.1016/j.immuni.2016.02.015.
15. Medzhitov R. Origin and physiological roles of inflammation. *Nature*. 2008;454:428–435. doi: 10.1038/nature07201.
16. Toulon A, Breton L, Taylor KR, Tenenhaus M, Bhavsar D, Lanigan C, Rudolph R, Jameson J, Havran WL. A role for human skin-resident T cells in wound healing. *J Exp Med*. 2009;206:743–750. doi: 10.1084/jem.20081787.
17. Rivollier A, He J, Kole A, Valatas V, Kelsall BL. Inflammation switches the differentiation program of Ly6Chi monocytes from antiinflammatory macrophages to inflammatory dendritic cells in the colon. *J Exp Med*. 2012;209:139–155. doi: 10.1084/jem.20101387.
18. Nathan C. Points of control in inflammation. *Nature*. 2002;420:846–852. doi: 10.1038/nature01320.
19. Mirza R, Koh TJ. Dysregulation of monocyte/macrophage phenotype in wounds of diabetic mice. *Cytokine*. 2011;56:256–264. doi: 10.1016/j.cyto.2011.06.016.
20. Khanna S, Biswas S, Shang Y, Collard E, Azad A, Kauh C, Bhasker V, Gordillo GM, Sen CK, Roy S. Macrophage dysfunction impairs resolution of inflammation in the wounds of diabetic mice. *PLoS One*. 2010;5:e9539. doi: 10.1371/journal.pone.0009539.
21. Willenborg S, Lucas T, van Loo G, Knipper JA, Krieg T, Haase I, Brachvogel B, Hammerschmidt M, Nagy A, Ferrara N, Pasparakis M, Eming SA. CCR2 recruits an inflammatory macrophage subpopulation critical for angiogenesis in tissue repair. *Blood*. 2012;120:613–625. doi: 10.1182/blood-2012-01-403386.
22. Auffray C, Sieweke MH, Geissmann F. Blood monocytes: development, heterogeneity, and relationship with dendritic cells. *Annu Rev Immunol*. 2009;27:669–692. doi: 10.1146/annurev.immunol.021908.132557.
23. Nahrendorf M, Swirski FK, Aikawa E, Stangenberg L, Wurdinger T, Figueiredo JL, Libby P, Weissleder R, Pittet MJ. The healing myocardium sequentially mobilizes two monocyte subsets with divergent and complementary functions. *J Exp Med*. 2007;204:3037–3047. doi: 10.1084/jem.20070885.
24. van Furth R, Cohn ZA. The origin and kinetics of mononuclear phagocytes. *J Exp Med*. 1968;128:415–435.
25. Taylor PR, Gordon S. Monocyte heterogeneity and innate immunity. *Immunity*. 2003;19:2–4.
26. Geissmann F, Manz MG, Jung S, Sieweke MH, Merad M, Ley K. Development of monocytes, macrophages, and dendritic cells. *Science*. 2010;327:656–661. doi: 10.1126/science.1178331.
27. Schulz C, Gomez Perdiguero E, Chorro L, Szabo-Rogers H, Cagnard N, Kierdorf K, Prinz M, Wu B, Jacobsen SE, Pollard JW, Frampton J, Liu KJ, Geissmann F. A lineage of myeloid cells independent of Myb and hematopoietic stem cells. *Science*. 2012;336:86–90. doi: 10.1126/science.1219179.
28. Serbina NV, Salazar-Mather TP, Biron CA, Kuziel WA, Pamer EG. TNF/iNOS-producing dendritic cells mediate innate immune defense against bacterial infection. *Immunity*. 2003;19:59–70.
29. Auffray C, Fogg D, Garfa M, Elain G, Join-Lambert O, Kayal S, Sarnacki S, Cumano A, Lauvau G, Geissmann F. Monitoring of blood vessels and tissues by a population of monocytes with patrolling behavior. *Science*. 2007;317:666–670. doi: 10.1126/science.1142883.
30. Zigmond E, Varol C, Farache J, Elmaliah E, Satpathy AT, Friedlander G, Mack M, Shpigel N, Boneca IG, Murphy KM, Shakhar G, Halpern Z, Jung S. Ly6C hi monocytes in the inflamed colon give rise to proinflammatory effector cells and migratory antigen-presenting cells. *Immunity*. 2012;37:1076–1090. doi: 10.1016/j.immuni.2012.08.026.
31. Yona S, Kim KW, Wolf Y, Mildner A, Varol D, Breker M, Strauss-Ayali D, Viukov S, Guilliams M, Misharin A, Hume DA, Perlman H, Malissen B, Zelzer E, Jung S. Fate mapping reveals origins and dynamics of monocytes and tissue macrophages under homeostasis. *Immunity*. 2013;38:79–91. doi: 10.1016/j.immuni.2012.12.001.
32. Dal-Secco D, Wang J, Zeng Z, Kolaczkowska E, Wong CH, Petri B, Ransohoff RM, Charo IF, Jenne CN, Kubes P. A dynamic spectrum of monocytes arising from the in situ reprogramming of CCR2+ monocytes at a site of sterile injury. *J Exp Med*. 2015;212:447–456. doi: 10.1084/jem.20141539.
33. Ferris ST, Zakharov PN, Wan X, Calderon B, Artyomov MN, Unanue ER, Carrero JA. The islet-resident macrophage is in an inflammatory state and senses microbial products in blood. *J Exp Med*. 2017;214:2369–2385. doi: 10.1084/jem.20170074.
34. Geissmann F, Jung S, Littman DR. Blood monocytes consist of two principal subsets with distinct migratory properties. *Immunity*. 2003;19:71–82.
35. Nahrendorf M, Pittet MJ, Swirski FK. Monocytes: protagonists of infarct inflammation and repair after myocardial infarction. *Circulation*. 2010;121:2437–2445. doi: 10.1161/CIRCULATIONAHA.109.916346.
36. Lauvau G, Chorro L, Spaulding E, Soudja SM. Inflammatory monocyte effector mechanisms. *Cell Immunol*. 2014;291:32–40. doi: 10.1016/j.cellimm.2014.07.007.
37. Passlick B, Flieger D, Ziegler-Heitbrock HW. Identification and characterization of a novel monocyte subpopulation in human peripheral blood. *Blood*. 1989;74:2527–2534.
38. Wong KL, Tai JJ, Wong WC, Han H, Sem X, Yeap WH, Kourilsky P, Wong SC. Gene expression profiling reveals the defining features of the classical, intermediate, and nonclassical human monocyte subsets. *Blood*. 2011;118:e16–e31. doi: 10.1182/blood-2010-12-326355.
39. Surwit RS, Kuhn CM, Cochrane C, McCubbin JA, Feinglos MN. Diet-induced type II diabetes in C57BL/6J mice. *Diabetes*. 1988;37:1163–1167.
40. Bolger AM, Lohse M, Usadel B. Trimmomatic: a flexible trimmer for Illumina sequence data. *Bioinformatics*. 2014;30:2114–2120. doi: 10.1093/bioinformatics/btu170.
41. Kim D, Langmead B, Salzberg SL. HISAT: a fast spliced aligner with low memory requirements. *Nat Methods*. 2015;12:357–360. doi: 10.1038/nmeth.3317.
42. Liao Y, Smyth GK, Shi W. featureCounts: an efficient general purpose program for assigning sequence reads to genomic features. *Bioinformatics*. 2014;30:923–930. doi: 10.1093/bioinformatics/btt656.
43. Robinson MD, McCarthy DJ, Smyth GK. edgeR: a Bioconductor package for differential expression analysis of digital gene expression data. *Bioinformatics*. 2010;26:139–140. doi: 10.1093/bioinformatics/btp616.

44. Piccolo V, Curina A, Genua M, Ghisletti S, Simonatto M, Sabò A, Amati B, Ostuni R, Natoli G. Opposing macrophage polarization programs show extensive epigenomic and transcriptional cross-talk. *Nat Immunol*. 2017;18:530–540. doi: 10.1038/ni.3710.
45. Jha AK, Huang SC, Sergushichev A, Lampropoulou V, Ivanova Y, Loginicheva E, Chmielewski K, Stewart KM, Ashall J, Everts B, Pearce EJ, Driggers EM, Artyomov MN. Network integration of parallel metabolic and transcriptional data reveals metabolic modules that regulate macrophage polarization. *Immunity*. 2015;42:419–430. doi: 10.1016/j.immuni.2015.02.005.
46. McCarthy DJ, Chen Y, Smyth GK. Differential expression analysis of multifactor RNA-Seq experiments with respect to biological variation. *Nucleic Acids Res*. 2012;40:4288–4297. doi: 10.1093/nar/gks042.
47. Dixit VD, Schaffer EM, Pyle RS, Collins GD, Sakthivel SK, Palaniappan R, Lillard JW Jr, Taub DD. Ghrelin inhibits leptin- and activation-induced proinflammatory cytokine expression by human monocytes and T cells. *J Clin Invest*. 2004;114:57–66. doi: 10.1172/JCI21134.
48. Lam QL, Lu L. Role of leptin in immunity. *Cell Mol Immunol*. 2007;4:1–13.
49. Chin CY, Monack DM, Nathan S. Delayed activation of host innate immune pathways in streptozotocin-induced diabetic hosts leads to more severe disease during infection with Burkholderia pseudomallei. *Immunology*. 2012;135:312–332. doi: 10.1111/j.1365-2567.2011.03544.x.
50. Swirski FK, Nahrendorf M, Etzrodt M, Wildgruber M, Cortez-Retamozo V, Panizzi P, Figueiredo JL, Kohler RH, Chudnovskiy A, Waterman P, Aikawa E, Mempel TR, Libby P, Weissleder R, Pittet MJ. Identification of splenic reservoir monocytes and their deployment to inflammatory sites. *Science*. 2009;325:612–616. doi: 10.1126/science.1175202.
51. Varol C, Vallon-Eberhard A, Elinav E, Aychek T, Shapira Y, Luche H, Fehling HJ, Hardt WD, Shakhar G, Jung S. Intestinal lamina propria dendritic cell subsets have different origin and functions. *Immunity*. 2009;31:502–512. doi: 10.1016/j.immuni.2009.06.025.
52. Kimball AS, Joshi A, Carson WF IV, Boniakowski AE, Schaller M, Allen R, Bermick J, Davis FM, Henke PK, Burant CF, Kunkel SL, Gallagher KA. The histone methyltransferase MLL1 directs macrophage-mediated inflammation in wound healing and is altered in a murine model of obesity and type 2 diabetes. *Diabetes*. 2017;66:2459–2471. doi: 10.2337/db17-0194.
53. Mirza RE, Fang MM, Weinheimer-Haus EM, Ennis WJ, Koh TJ. Sustained inflammasome activity in macrophages impairs wound healing in type 2 diabetic humans and mice. *Diabetes*. 2014;63:1103–1114. doi: 10.2337/db13-0927.
54. Dunay IR, Damatta RA, Fux B, Presti R, Greco S, Colonna M, Sibley LD. Gr1(+) inflammatory monocytes are required for mucosal resistance to the pathogen Toxoplasma gondii. *Immunity*. 2008;29:306–317. doi: 10.1016/j.immuni.2008.05.019.
55. Rose S, Misharin A, Perlman H. A novel Ly6C/Ly6G-based strategy to analyze the mouse splenic myeloid compartment. *Cytometry A*. 2012;81:343–350. doi: 10.1002/cyto.a.22012.
56. Tsou CL, Peters W, Si Y, Slaymaker S, Aslanian AM, Weisberg SP, Mack M, Charo IF. Critical roles for CCR2 and MCP-3 in monocyte mobilization from bone marrow and recruitment to inflammatory sites. *J Clin Invest*. 2007;117:902–909. doi: 10.1172/JCI29919.
57. Olingy CE, San Emeterio CL, Ogle ME, Krieger JR, Bruce AC, Pfau DD, Jordan BT, Peirce SM, Botchwey EA. Non-classical monocytes are biased progenitors of wound healing macrophages during soft tissue injury. *Sci Rep*. 2017;7:447. doi: 10.1038/s41598-017-00477-1.
58. Cipolletta C, Ryan KE, Hanna EV, Trimble ER. Activation of peripheral blood CD14+ monocytes occurs in diabetes. *Diabetes*. 2005;54:2779–2786.

Highlights

- Blood CD11b^{+}Ly6C^{Hi} monocytes profoundly influence both normal and pathological wound healing.
- In normal wounds, CD11b^{+}Ly6C^{Hi} cells are the predominant subset early postinjury, followed by a transition to a CD11b^{+}Ly6C^{Lo}-dominant phenotype; however, in diabetic wounds there was a second influx of recruited CD11b^{+}Ly6C^{Hi} monocytes, that corresponded with increased tissue MCP-1 (monocyte chemoattractant protein-1).
- Adoptive transfer of fluorescent *tdTomato*-labeled CD11b^{+}Ly6C^{Hi} monocytes demonstrated that diabetic CD11b^{+}Ly6C^{Hi} monocytes have a delayed phenotypic switch to CD11b^{+}Ly6C^{Lo} cells.
- Based on transcriptome profiling of flow-sorted wound CD11b^{+}Ly6C^{Hi} and CD11b^{+}Ly6C^{Lo} cells, we found that CD11b^{+}Ly6C^{Hi} monocyte-macrophages from diabetic wounds differ significantly in their expression of proinflammatory and profibrotic genes.
- Timed administration of anti-MCP-1 antibody prevents the second influx of CD11b^{+}Ly6C^{Hi} monocytes and reverses impaired diabetic wound healing.